

Cosurfactant and cosolvent effects on surfactant self-assembly in supercritical carbon dioxide

Naresh Chennamsetty,^{a)} Henry Bock, Lauriane F. Scanu, Flor R. Siperstein,^{b)} and Keith E. Gubbins

Department of Chemical and Biomolecular Engineering, North Carolina State University, Raleigh, North Carolina 27695-7905

(Received 12 August 2004; accepted 9 December 2004; published online 28 February 2005)

The impact of alcohol additives on the self-assembly of surfactants in supercritical carbon dioxide is investigated using lattice Monte Carlo simulations. We observe that all studied (model) alcohols reduce the critical micelle concentration. The reduction is stronger the longer the hydrocarbon chain of the alcohol, and the higher the alcohol concentration. Short-chain alcohols are found to concentrate in the surfactant layer of the aggregates, replacing surfactant molecules and leading to a strong decrease of the aggregation number and a large increase of the number of aggregates. On the other hand, only a small number of alcohol molecules with longer chain length are found in the aggregates, leading to a slight increase in the aggregation number. However, structural properties such as size and density profiles of aggregates at the same aggregation number are not influenced markedly. Consequently, short-chain alcohols act as *cosurfactants*, directly influencing the properties of the aggregates, while alcohols with longer hydrocarbon chains work as *cosolvents*, altering the properties of the solvent. However, the transition between both extremes is gradual. © 2005 American Institute of Physics. [DOI: 10.1063/1.1855291]

I. INTRODUCTION

Supercritical carbon dioxide (scCO₂) is an attractive alternative to conventional solvents since it is environmentally benign, inexpensive, essentially nontoxic, and has moderate critical conditions ($T_C=304.13$ K, $P_C=73.773$ bar). Furthermore, its density, viscosity, and dielectric properties are unusually tunable by small changes in the thermodynamic conditions (temperature and pressure), which are easy to control in practice, making supercritical carbon dioxide an unusually versatile solvent.¹ Unfortunately, the poor solvent quality of CO₂ for polar substances (such as water and ionic compounds) and high molecular weight polymers limits its wide application. One potential way to overcome this limitation is to solubilize these otherwise insoluble substances within reverse micelles formed by surfactants.²⁻⁴ However, the low solvent strength of CO₂ also limits the solubility of many surfactants, which in turn prevents sufficient solubilization of hydrophilic substances.⁵ This situation can be substantially improved by adding cosurfactants or cosolvents such as alcohols.⁶⁻¹⁰

Surprisingly less work has been done on the effect of alcohol additives in supercritical CO₂. Liu *et al.*⁹ showed that adding n-pentanol leads to an increase of the solubility of the primary surfactant (tetraethylene glycol n-lauryl ether, H[CH₂]₁₂[OCH₂CH₂]₄OH, i.e., C₁₂E₄, where C=methylene or methyl and E=ethylene oxide) with increasing alcohol concentration at all temperatures and CO₂ pressures studied.

Under constant CO₂ pressure conditions, an alcohol concentration of 1.12 M caused a fourfold increase of the C₁₂E₄ solubility. In a similar system, McFann *et al.*^{6,7} studied the solubility of water and found that 0.5–0.8 wt. % water can be solubilized in a solution of pentaethylene glycol n-octyl ether (C₈E₅) in scCO₂, depending on the surfactant concentration. The water load of the solution was found to increase by a factor of 4 to 5 if n-pentanol was added.

Later, Sawada *et al.*⁸ studied the same system and systematically investigated the dependence of the solubility of C₈E₅ on the chain length of the added alcohol. The solubility experiments revealed an optimum performance of the alcohol with a chain length of 5 carbon atoms, i.e., n-pentanol. The authors⁸ further report that this behavior was independent of temperature. In agreement with McFann's results, Sawada *et al.* also found that the water solubility increased significantly with increasing n-pentanol concentration.

The solubility of the nonionic surfactant Ls-54 in supercritical CO₂ was investigated by Liu *et al.*¹⁰ The addition of n-propanol, n-pentanol, or n-heptanol decreased the cloud point pressure (CPP) of the Ls-54/scCO₂ system, i.e., at constant CO₂ pressure, the solubility of Ls-54 was increased. The largest reduction of the CPP was measured for n-propanol. On the contrary, benzyl alcohol *increased* the cloud point pressure, *reducing* the solubility of Ls-54.

Far more studies on the effect of alcohols have been carried out in water/surfactant/oil systems. In these systems it is usually desired to find a surfactant, which at given thermodynamic conditions and for a given oil, stabilizes a microemulsion middle phase rather than water-in-oil or oil-in-water microemulsions. Winsor¹¹ found that the performance of the surfactant depends on the balance between surfactant–

^{a)}Electronic mail: nchenna@unity.ncsu.edu

^{b)}Present address: Department d'Enginyeria Química, Universitat Rovira i Virgili, Campus Sescelades, Av. dels Països Catalans, 26, 43007, Tarragona, Spain.

oil and surfactant–water interactions.¹² To achieve optimal performance, it may require surfactant molecules with long hydrophobic tails. However, if the surfactant tail becomes too long, the solubility of the surfactant in water may decrease to a value below the critical micelle concentration (CMC), such that neither micelles nor microemulsions can form.¹³ As in the CO₂ systems, alcohol additives successfully stabilize microemulsions in water/surfactant/oil systems.^{14–17} Alcohols can also decrease the CMC, depending on alcohol concentration and tail length.^{18–20} Some authors suggest that the alcohol molecules operate by inserting themselves between the surfactant tails, reducing tail–tail and micelle–micelle interactions,^{21–23} while others argue that they act at the interface itself, reducing the surface tension.^{24,25} Another view is that the additives distribute mainly between the aqueous and the oil phases, altering the solvent properties.²⁶

These assumptions about the function of the additives led to a classification into two groups: *cosolvents* and *cosurfactants*. Cosurfactants are weakly amphiphilic molecules, which are assumed to concentrate in the surfactant layer of the aggregates formed by the primary surfactant. Due to their weak amphiphilic character, cosurfactants alone do not form aggregates, but they strongly support aggregation of the primary surfactant. Common examples of cosurfactants are medium chain alcohols (5–8 carbon units). Cosolvents, on the other hand, are not necessarily amphiphilic. In CO₂ systems, their main function is to improve the solvent quality of CO₂. This is necessary since hydrocarbons are not very soluble in CO₂, preventing the solubilization of surfactants with hydrocarbon tails. Fluorocarbon surfactants are much more soluble in CO₂ than hydrocarbon surfactants, but their use is questionable, since the entire solution should be environmentally friendly.

Frequently the same molecules (alcohols) are considered as cosurfactants and cosolvents. One reason is that it is very difficult to directly measure the composition of the surfactant layer. Usually theories are fitted to the experimental results, which in turn indicate the distribution of the additive in the system.²⁰ In NMR measurements of a water-in-oil (n-hexane) microemulsion, a more direct observation of the distribution of additive molecules was made.²⁷ A large amount of cosurfactant (n-pentanol) was found at the microemulsion interface, thus qualifying n-pentanol as cosurfactant for this system. However, it must be assumed that for many additives there is no clear-cut distinction between cosurfactants and cosolvents. Additive molecules will be present in the surfactant layer as well as in the surrounding solution, thus altering the properties of the solvent as well as those of the surfactant layer.

While molecular properties such as the distribution of additive molecules are usually difficult to measure experimentally, they are natural observables in molecular simulations. Thus, lattice and off-lattice simulation methods have been used to study the self-assembly and phase behavior of surfactants in supercritical carbon dioxide.^{28–33}

Off-lattice simulations are very attractive since they provide an association of the thermodynamic properties of the system with very detailed molecular information, at least in principle. Salaniwal *et al.*^{28,29} used a hybrid full-atom/united-

atom model in molecular dynamics (MD) simulations to study reverse micelles formed in a CO₂/dichain surfactant/water system. One of their systems, containing 33 surfactants, was observed over a period of 1 ns. During this time one aggregate formed from a preassembled starting configuration. The size and shape of the aggregate was in reasonable agreement with experimental findings. The enclosed water in the center of the reverse micelle showed dramatic structural differences from the water located close to the surfactant head groups. A similar system was investigated by Senapati *et al.*³⁰ using united-atom molecular dynamics simulations. In their system, 160 dichain fluorosurfactant molecules stabilized one microemulsion droplet, which was observed over a period of 4 ns. The radius of gyration of the droplet was in reasonable agreement with small-angle neutron scattering (SANS) experiments at the same thermodynamic conditions. A small section of a surfactant stabilized CO₂/water interface was studied by da Rocha and co-workers employing full-atomistic MD simulations.³¹ As these examples show, off-lattice simulations are invaluable tools to investigate CO₂/surfactant/water systems, but they are challenging because of the various length and time scales involved. Consequently they are usually limited to relatively small systems and short times.

In this paper we are interested in thermodynamic equilibrium properties of surfactant solutions. This requires much larger systems than in the examples above, where single-aggregate properties were investigated. To achieve the required system sizes, it is necessary to “trade” a detailed description of the molecules for a coarse-grained model of the system. Coarse models are commonly used in stochastic dynamics methods such as Brownian dynamics (BD) or dissipative particle dynamics (DPD). Using DPD, Rekvig *et al.*³⁴ studied the impact of mixing different surfactants on the bending modulus of a surfactant stabilized water/oil interface. They observed that mixing long- and short-chain surfactants leads to more flexible interfaces compared to usage of surfactants with a chain length intermediate between the long and the short one.

Alternative coarse-grained models are applied in lattice Monte Carlo simulations of surfactant systems. Recently, Zaldivar and Larson³⁵ studied the aggregation behavior of binary mixed micelles in an incompressible solvent using lattice Monte Carlo simulations. In their model, the two surfactant species are distinguished by the difference in the unlike surfactant head/head interaction compared to the like surfactant head/head interaction. They observed a synergistic lowering of the CMC for surfactant mixtures with an effective unlike surfactant head/head net attraction, and an increase in the opposite case. An optimum was found when both surfactant species have the same concentration in the solution. The lattice model originally developed by Larson^{36–38} has been modified for compressible fluids by Lisal *et al.*^{32,39} to study surfactant solutions in supercritical carbon dioxide, and used by Scanu *et al.*³³ to reproduce the correct CO₂ density dependence of the critical micelle concentration (CMC).

In this work, we use lattice Monte Carlo simulations to study the effect of alcohols on the micellization of surfac-

tants in supercritical CO₂. Special attention is drawn to the location of additive molecules in the system. Further, we study the dependence of the CMC and the size, shape, and structure of the micelles as a function of alcohol chain length and alcohol concentration. We also discuss how increasing the alcohol chain length changes the additive behavior from cosurfactant to cosolvent.

The remainder of this paper is organized as follows: In Sec. II, we describe the model and give definitions of the properties that characterize the micellar solution. Section III is devoted to a presentation of our results. We analyze our results in two parts: The first part is concerned with the formation of the aggregates, while the second part investigates structural properties, shape, size, and density distributions. Finally, we summarize our findings and conclusions in Sec. IV.

II. MODEL AND SIMULATION

Throughout we use *reduced quantities*: all lengths are reduced with the lattice constant, ℓ , the energy scale is given in units of the absolute value of the CO₂/CO₂ interaction energy, $|\varepsilon_{CC}|$, and the temperature is reduced with $k_B/|\varepsilon_{CC}|$, where k_B is the Boltzmann constant.

A. Model

To study surfactant solutions in supercritical CO₂-containing additive molecules, we employ a modified version of Larson's lattice model^{36–38} proposed by Lisal *et al.*³² This model allows vacant lattice sites leading to a non-vanishing compressibility, which is essential to correctly describe supercritical fluids such as CO₂.^{32,33} In the lattice model, CO₂ molecules are represented by single beads and surfactant, and additive molecules by chains of beads. The bead positions are restricted to the sites of a simple cubic lattice with lattice constant ℓ . Each bead interacts with its nearest neighbors and with neighbors that are $\sqrt{2}\ell$ and $\sqrt{3}\ell$ apart, giving a total coordination number of 26. The same vectors that connect interacting beads also connect consecutive beads in the chain molecules. The surfactant used here is denoted by H_5T_4 , consisting of 5 head beads (H) and 4 tail beads (T), occupying a total of 9 lattice sites. This model molecule could represent a member of the widely used non-ionic ethylene glycol surfactants, e.g., tetraethylene glycol n-octyl ether (C₈E₄), which has four ethylene oxide groups and one terminal OH group. Similarly, the additive molecules are denoted by ht_α , consisting of one head bead (h) and α tail beads (t), giving a total of $1+\alpha$ beads. We assume that these additive molecules represent a homologous series of linear alcohols with one terminal OH group. Head and tail groups of the model molecules are distinguished by their interaction energies with other beads in the system. In our definition, we follow the common convention that the head groups are hydrophilic, i.e., CO₂-phobic, and the tail groups are hydrophobic, i.e., CO₂-philic. Thus, in CO₂, the surfactants form *reverse micelles* (head inside, tail outside). However, for the sake of simplicity and convenience we will refer to them as “micelles.”

TABLE I. Interaction energies between CO₂ (C), surfactant head, (H), surfactant tail (T), alcohol head (h), and alcohol tail (t). The surfactant/CO₂ interaction energies are taken from Ref. 33. Here, ε_{ab} denotes the interaction energy between different species a and b , where a and b represent H , T , h , t , or C and w_{ab} denotes the exchange energy [see Eq. (1)].

Like interactions		Unlike interactions		
Type of interaction	ε_{ab}	Type of interaction	ε_{ab}	w_{ab}
$C-C$	-1	$C-H$, $C-h$	-1	1
$H-H$, $h-h$	-3	$C-T$, $C-t$	-3	-2
$T-T$, $t-t$	-1	$H-h$	-4	-1
		$T-t$	-1	0
		$H-T$, $H-t$, $h-T$, $h-t$	-1	1

The set of interaction energies used in this study is given in Table I. The surfactant/CO₂ interaction parameters are taken from Ref. 33. The peculiarity of this set of interaction energies is that it correctly reproduces the experimental trends of the CMC with CO₂ density,³³ while others do not.³² We choose the interaction energies of the alcohols to be equal to those of the surfactant. The exchange energy between the alcohol head group and the surfactant head group is set to $w_{Hh}=-1$.

Exchange energies are convenient tools to characterize mixing tendencies in the solution. The exchange energy, w_{ab} , is defined as

$$w_{ab} = \varepsilon_{ab} - \frac{\varepsilon_{aa} + \varepsilon_{bb}}{2}, \quad a \neq b. \quad (1)$$

Although the interaction energy between CO₂ and surfactant heads is attractive, $\varepsilon_{CH}=-1$, the corresponding exchange energy is repulsive, $w_{CH}=1$. Thus, they repel each other because of the strong H/H attraction ($\varepsilon_{HH}=-3$). The mild repulsion of the phobic exchange energies ($w_{CH}=w_{TH}=1$) ensures that the CMC does not occur at too low a surfactant concentration.³³

B. Monte Carlo simulations

We study the thermodynamic behavior of the lattice model described above using lattice Monte Carlo simulations in the canonical ensemble (NVT). In order to avoid finite size effects on the aggregation behavior, we simulate systems accommodating 5 to 10 micelles. This requires lattice sizes ranging from $N=40^3$ (for higher surfactant concentrations) up to $N=130^3$ lattice sites (for lower surfactant concentrations near the CMC). These N lattice sites are occupied by N_C CO₂ beads, $9N_{H_5T_4}$ surfactant beads, and $(1+\alpha)N_{ht\alpha}$ alcohol beads. Consequently, $N_v=N-[N_C+9N_{H_5T_4}+(1+\alpha)N_{ht\alpha}]$ lattice sites are vacant. Periodic boundary conditions are applied in all three dimensions.

To efficiently sample configuration space, we use *complete chain regrowth* with configurational bias, *reptation*, and *twist* moves for surfactant and alcohol molecules and *particle exchange* (switch) moves for CO₂, where we attempt to move a CO₂ bead to a randomly chosen vacant site.⁴⁰ We typically run 1×10^5 to 2×10^5 cycles for equilibration and 4×10^5 to 8×10^5 cycles for evaluation of quantities of interest. Each cycle consists of N_C+N_v switch moves, $9N_{H_5T_4}$

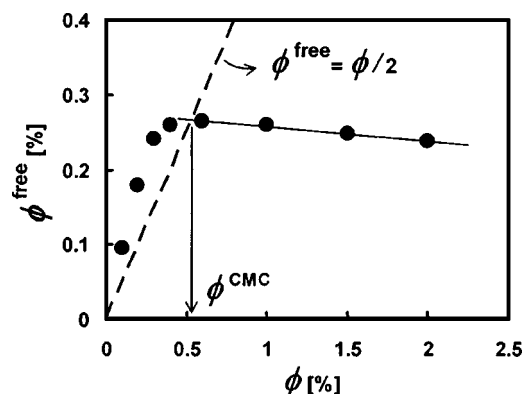


FIG. 1. Determination of the CMC for a solution of surfactant H_5T_4 in $scCO_2$ containing 5% alcohol ht . The solid line is a linear fit to the simulation results at $\phi \geq 0.6\%$.

chain moves for the surfactants, and $(1 + \alpha)N_{ht\alpha}$ chain moves for the alcohol molecules. In each chain move, a molecule is randomly selected and a randomly chosen move (regrowth, reptation, and twist) is performed. The different chain moves are chosen with equal probability.

In solution, surfactant molecules aggregate spontaneously. A surfactant (or additive) molecule is defined to belong to a specific aggregate if one of its head beads is a neighbor of a head bead of a surfactant (or additive) molecule that belongs to the same aggregate. A surfactant molecule is called “free” if it does not belong to any aggregate. In the simulations we determine aggregates using the *cluster multiple labeling technique* of Hoshen and Kopelman.⁴¹

C. Thermodynamic properties

During the simulation, we monitor several quantities such as the fraction of free surfactants, the aggregation number distribution, the radii of gyration of micelles, and the density profile within a micelle. In this section we present the definitions of these properties that we will use throughout the paper.

1. Concentration

To quantify the content of the solution we use volume fractions, ϕ , in [%], henceforth called “concentration.” In our lattice model, volume fractions are identical to site fractions, since *a priori* all beads have the same volume.

2. Critical micelle concentration

At low surfactant concentrations, individual surfactant molecules are dissolved in the solvent, while micelles form at higher concentrations. The threshold concentration where the first micelles appear in the system is called *critical micelle concentration* (CMC). Unfortunately, the CMC is not an *a priori* well-defined point. While several definitions of the CMC exist and give similar results,^{42–48} we employ the definition given by Israelachvili *et al.*⁴² In Fig. 1, we present a typical plot of the concentration of free surfactant molecules, ϕ^{free} , as a function of the total surfactant concentration, ϕ , at 5% alcohol ht . Although the alcohol might influence the value of the CMC, it is not involved in CMC

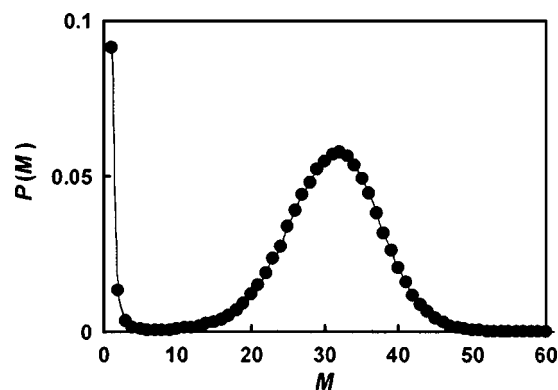


FIG. 2. Surfactant aggregation number distribution at 2.5% surfactant H_5T_4 and 5% alcohol ht .

determination. According to Israelachvili’s definition, the CMC is given by the surfactant concentration where the line $\phi^{\text{free}} = \phi/2$ (dashed line) intersects the line representing a fit to the linear part of the curve at high surfactant concentration (solid line). The CMC thus calculated is $\phi^{\text{CMC}} = 0.54\%$. We note that according to this definition $\phi^{\text{free}} = \phi^{\text{CMC}}/2$ at the CMC.

3. Aggregation number distribution

Micelles are dynamic entities with surfactant molecules entering and leaving over the course of their “lifetime.” Therefore, surfactant solutions comprise aggregates of different aggregation numbers, M , quantified by aggregation number distributions. The commonly used aggregation number distribution, $P(M)$, which represents the fraction of surfactant molecules bound in aggregates of size M , is defined as

$$P(M) = \frac{MN_M}{\sum_M MN_M} = \frac{MN_M}{N_{H_5T_4}}, \quad (2)$$

where N_M is the ensemble average of the number of aggregates of aggregation number M and $N_{H_5T_4}$ is the total number of H_5T_4 surfactant molecules. In Fig. 2, a typical surfactant aggregation number distribution is shown, which is obtained at 2.5% H_5T_4 and 5% ht . It comprises a steeply rising part when M approaches 1, and the usual bell-shaped maximum, separated by a minimum. The symmetry of the aggregate size distribution suggests that a mean aggregation number \bar{M} can be defined by

$$\bar{M} = \frac{\sum_{M>5} MN_M}{\sum_{M>5} N_M}. \quad (3)$$

Note that free surfactants ($M=1$) and small aggregates ($2 \leq M \leq 5$) are excluded from the calculation of \bar{M} .

4. Radius of gyration

Convenient measures of the shape of micelles are the three “principal radii of gyration,” which are obtained in the following way: At first one calculates the instantaneous gyration tensor, \underline{R} , defined by⁴⁹

$$R_{kl}^2 = \frac{1}{n} \sum_{i=1}^n [r_k(i) - r_k^*][r_l(i) - r_l^*], \quad (4)$$

for each micelle. The sum in (4) runs over the n beads of all surfactant molecules which belong to the micelle, $r_k(i)$ and $r_l(i)$ are the (x, y, z) components of the position vector, $\underline{r}(i)$, of bead i and \underline{r}^* is the position of the center of mass. We note that this definition implies the head and tail beads have the same mass. Next, the three eigenvalues of \underline{R} are determined and ordered, $\hat{R}_1 \leq \hat{R}_2 \leq \hat{R}_3$. These eigenvalues represent the principal radii of gyration of the micelle under consideration. A micelle is considered spherical if $\hat{R}_1 = \hat{R}_2 = \hat{R}_3$. The properties which are commonly called “principal radii of gyration of micelles with aggregation number M ” are given by

$$R_\beta(M) = \langle \hat{R}_\beta(M) \rangle, \quad \beta = 1, 2, 3, \quad (5)$$

where $\langle \rangle$ denotes the ensemble average. By considering only the head beads one obtains the principal radii of gyration of the core of the reverse micelles, $R_\beta^C(M)$. By averaging the principal radii of gyration, one obtains the mean radius of gyration, $R(M)$

$$R(M) = \frac{1}{3} \sum_{\beta=1}^3 R_\beta(M). \quad (6)$$

Values of $R(M)$ obtained in solutions at different thermodynamic conditions can be used to compare the size of micelles of aggregation number, M . At constant M , a larger value of $R(M)$ indicates that the micelle extends further into the solvent compared to a micelle with a smaller $R(M)$.

5. Density profile

The structure within spherical micelles can be analyzed using radial density profiles for each species of beads $a = H, T, h, t, C, v$. The density profile, $n_a(r)$, of a particular species, a , is defined as

$$n_a(r) = \frac{\langle N_a(r) \rangle_M}{N_{\text{total}}(r)}, \quad (7)$$

where $\langle \rangle_M$ denotes the ensemble average for all micelles of aggregation number M , $N_a(r)$ is the number of lattice sites occupied by beads of species a at a distance r from the center of mass, and $N_{\text{total}}(r)$ stands for the total number of lattice sites at this distance r . We note that $n_a(r)$ depends also on M , although we do not show this explicitly.

6. Connection to experiments

Our simulations are carried out at constant (reduced) temperature, $T=6.4$ and constant CO₂ (reduced) number density $\rho=0.86$. These conditions correspond to the experimental conditions of McFann *et al.*⁷ discussed in the Introduction.

Using corresponding state theory for the pure solvent, we can relate the reduced temperature to an explicit temperature in kelvin, through the ratio

$$\frac{T}{T_C} = \frac{T[\text{K}]}{T_C[\text{K}]}, \quad (8)$$

where T is the temperature in the present model, $T_C=5.85$ is the critical temperature of the model,^{50,51} $T[\text{K}]$ is the corresponding temperature in kelvin, and $T_C[\text{K}]=304.13$ K is the measured critical temperature of CO₂. From Eq. (8), we estimate that the reduced temperature, $T=6.4$, corresponds to $T[\text{K}]=333$ K in pure CO₂.

In an analogous way, one estimates the density of the pure solvent.³² For the densities, corresponding states theory requires

$$\frac{\rho}{\rho_C} = \frac{\rho[\text{g/ml}]}{\rho_C[\text{g/ml}]}, \quad (9)$$

where ρ is the volume fraction of CO₂ in the model, $\rho[\text{g/ml}]$ is the corresponding density in explicit units, $\rho_C=0.5$ is the critical density of the model, and $\rho_C[\text{g/ml}]=0.4676$ g/ml is the experimentally measured critical density of CO₂. Thus, the reduced number density (or volume fraction) of the pure solvent, $\rho=0.86$, corresponds to $\rho[\text{g/ml}]=0.8$ g/ml. We note that within the present model the *reduced* number density of CO₂ and the CO₂ volume fraction are equivalent.

III. RESULTS

We investigate the impact of concentration and architecture of alcohols, ht_α , on the aggregation behavior of the surfactant H_5T_4 in supercritical CO₂. All simulations are carried out at constant temperature, $T=6.4$ and constant CO₂ density $\rho=0.86$. Here, ρ is calculated by counting only lattice sites that are *not* occupied by surfactant or additive molecules, i.e., vacancy and CO₂. We assume that the solvent quality of CO₂ is constant as long as ρ is kept constant. We maintain constant solvent quality so as not to bias the interpretation of the effect of adding alcohols by a simultaneous change of the solvent quality.

A. Formation of aggregates

A characteristic property of surfactant aggregation in bulk solutions is the *critical micelle concentration* (CMC). The dependence of the CMC of H_5T_4 surfactants on the concentration of two different alcohols, ht and ht_4 , in supercritical CO₂, is shown in Fig. 3(a). The addition of alcohol leads to a reduction of the CMC in both cases. Thus, both alcohols support aggregation of the surfactant. The CMC decreases monotonously with increasing concentration of alcohol. The decrease becomes weaker as the alcohol concentration increases. In the case of ht , addition of alcohol beyond 2.5% has essentially no effect on the CMC. In general, the effect of the alcohol having the longer tail group is much stronger than that of the shorter one. An alcohol concentration of 10% ht_4 lowers the CMC by a factor of 3, while 10% ht lowers it by less than 10%. The dependence of the CMC of H_5T_4 surfactants on the alcohol chain length is shown in Fig. 3(b). We observe that increasing the length of the alcohol at constant alcohol concentration decreases the CMC monotonously. However, the decrease becomes weaker for $\alpha > 3$.

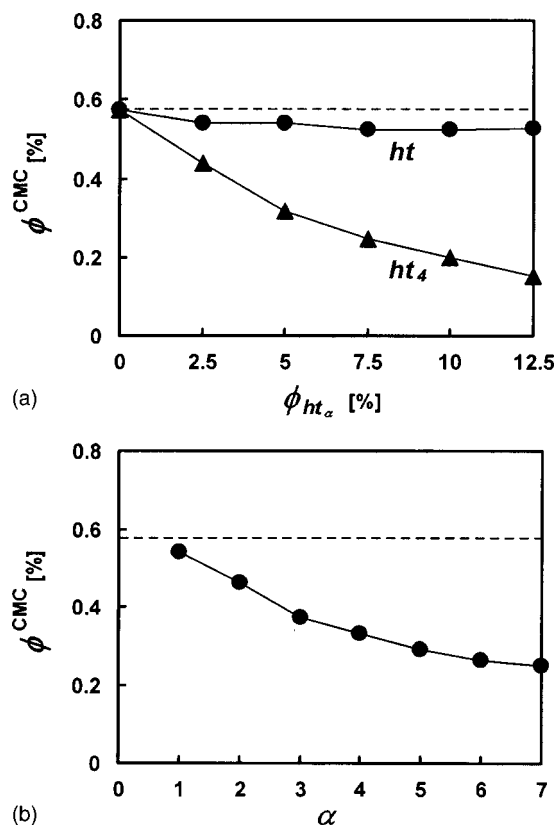


FIG. 3. (a) CMC of surfactant H_5T_4 as a function of concentrations of alcohols ht and ht_4 . (b) CMC of surfactant H_5T_4 as a function of the chain length of the alcohol (ht to ht_7) at constant alcohol concentration of 5%. In parts (a) and (b), the dashed lines indicate the CMC of pure H_5T_4 surfactant without any alcohol, and solid lines are drawn to guide the eye.

To our knowledge, no experimental data for the dependence of CMC on alcohol type and concentration are available in the literature for surfactant solutions in supercritical CO_2 . In Fig. 4, we present experimental CMC values for an aqueous solution of potassium dodecanoate as a function of alcohol type and concentration.¹⁸ Both experiments (in H_2O) and simulations (in CO_2) have been carried out at constant thermodynamic conditions of the solvent, so that a qualitative comparison is possible. Comparison of Figs. 3 and 4 reveals that in both simulation and experiment the impact of the longer alcohols is always stronger than that of the shorter ones, and that the effect is stronger the higher the alcohol

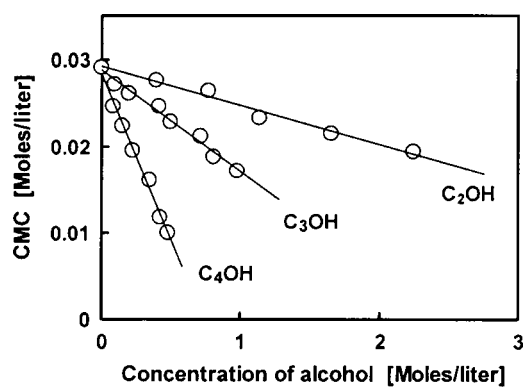


FIG. 4. The effect of ethanol, propanol, and butanol on the CMC of potassium dodecanoate in water at 10 °C. Data taken from Ref. 18.

concentration. It is interesting to notice that, although the behavior of the CMC in the two solvents is very similar, the structure of the two systems is quite different. While we observe reverse micelles in the simulations of the CO_2 system, regular micelles are formed in aqueous solutions. Thus, the mechanism by which the CMC is lowered might be quite different in the two cases.

The results plotted in Fig. 3 clearly show that the addition of alcohols lowers the CMC, and that their performance depends on concentration and chain length. Using the detailed molecular information available from our simulations, we now investigate the cause of these effects. We first study the effect of the concentration of alcohol ht on the mean aggregation number, \bar{M} , and on the composition of the micelles. In Fig. 5(a), the mean aggregation number of H_5T_4 micelles and the average number of ht molecules present in micelles with an aggregation number, $M = \bar{M}$, are plotted as a function of ht concentration at 2.5% H_5T_4 . The pure H_5T_4/CO_2 system at this surfactant concentration consists of micelles with $\bar{M} = 40$. Addition of ht drastically decreases the mean aggregation number until, at 10% ht , the value of \bar{M} is half that of the pure system. This large reduction in the number of H_5T_4 molecules per micelle seems to be compensated by binding of ht molecules in micelles. Results from Fig. 5(a) indicate that each H_5T_4 molecule leaving the micelle is replaced by approximately two alcohol ht molecules.

The large effect of ht on the aggregation number is surprising since the CMC is only lowered slightly. In contrast, the impact of ht_4 on the CMC is large but the aggregation number *increases* with increasing ht_4 concentration [Fig. 5(b)] and only a few ht_4 molecules “enter” the micelles. From the plot in Fig. 5(c), we observe that ht strongly decreases the mean aggregation number of H_5T_4 micelles. However, increasing the alcohol tail length, α , continuously increases the aggregation number, such that for $\alpha > 2$ the mean aggregation number of the (10%) alcohol-containing solution exceeds \bar{M} of the solution without alcohol. The average number of alcohol molecules bound in micelles is large for the ht containing system but it decreases rapidly as α increases.

Since addition of ht molecules does not lower the CMC significantly, and the concentration of free surfactant molecules is approximately half the CMC (Fig. 1), the number of surfactant molecules bound in micelles remains almost unchanged. On the other hand, addition of 10% ht halves the aggregation number. Consequently one expects the number of aggregates to increase by a factor of 2. The addition of ht_4 leads to a lower CMC, i.e., more surfactant molecules are bound in micelles compared to the system without alcohol. On the other hand, addition of ht_4 increases the mean aggregation number. While a lower CMC leads to a higher number of aggregates, the increase of the mean aggregation number is reducing it. These two small opposing effects may compensate one another, i.e., one expects the number of aggregates in the solution with 10% ht_4 to be roughly equal to the one in the pure H_5T_4 solution.

In Fig. 6, we present the aggregation number distributions, $P(M)$, defined in Eq. (2), for H_5T_4 solution at different

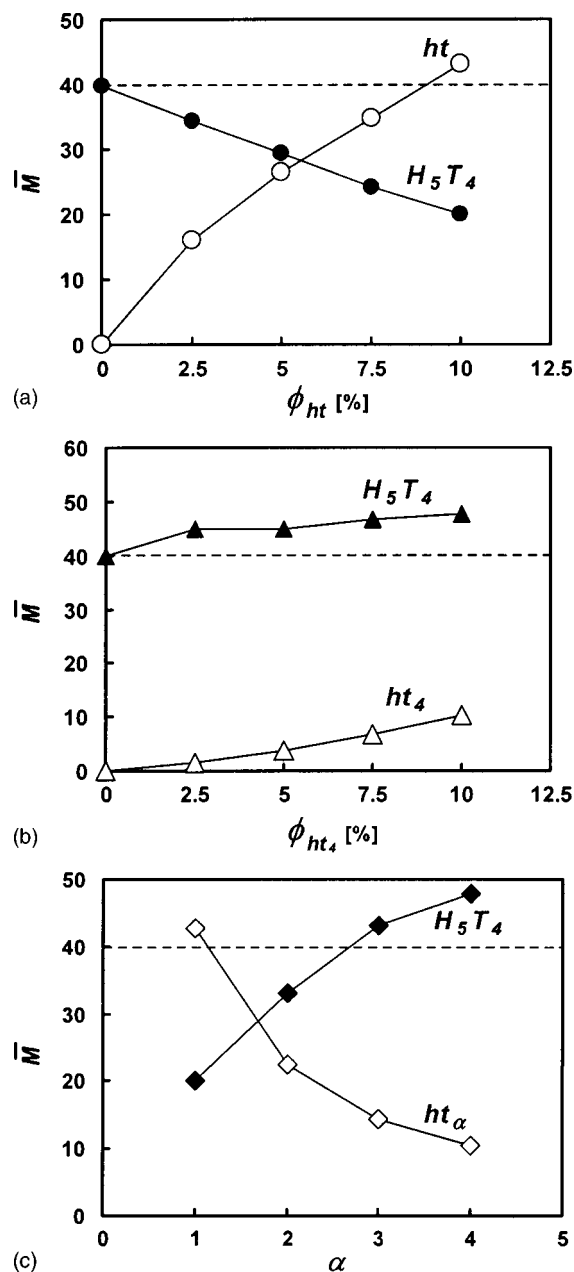


FIG. 5. (a) Mean aggregation number of H_5T_4 micelles (filled symbols) and the average number of ht molecules within micelles with aggregation number $M = \bar{M}$ (open symbols) as a function of ht concentration at 2.5% H_5T_4 . The dashed line indicates the mean aggregation number of H_5T_4 micelles formed in CO₂ without alcohol. Solid lines are drawn through the data as a guide to the eye. (b) Same as (a) but for ht_4 . (c) Same as (a) but as a function of alcohol chain length at 10% alcohol concentration.

ht concentrations. As the concentration of ht molecules increases, the bell-shaped part of the curve shifts to lower aggregation numbers while the shape and height do not change markedly. Since the area below the bell-shaped part of the curves is proportional to the number of surfactant molecules bound in micelles, the plots in Fig. 6 are consistent with the observation that the CMC is only weakly influenced by the addition of ht [Fig. 3(a)].

The distribution of the number of aggregates per H_5T_4 molecule, $P^*(M) = P(M)/M$, for the pure H_5T_4 solution and for the solutions containing 10% ht and 10% ht_4 , is shown in Fig. 7. The maximum of the curve for the solution containing

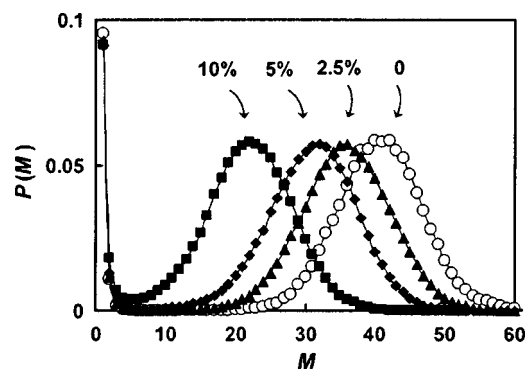


FIG. 6. Surfactant aggregation number distributions for 2.5% H_5T_4 solution at different ht concentrations (0%, 2.5%, 5%, 10%).

10% ht is about twice as high as the maximum of P^* for the pure H_5T_4 solution. Thus, addition of 10% ht doubles the number of micelles but halves their mean aggregation number compared to the system without alcohol. The addition of 10% ht_4 , on the other hand, leads to a slight increase of the aggregation number, while the height of the maximum of P^* is slightly decreased. The lowering of the maximum is accompanied by a broadening of P^* . Both effects compensate each other, such that the integral of the Gaussian part of P^* is almost identical for the solution containing 10% ht_4 and for the pure H_5T_4 solution. Thus, addition of 10% ht_4 does not change the number of micelles, although it slightly increases the mean aggregation number. Consequently, more surfactant molecules are bound in micelles and the CMC must decrease, which is consistent with our findings presented in Fig. 3(a).

These observations are quite intriguing since they show that the two molecules ht and ht_4 , which are very similar in structure, can have very different effects on the behavior of H_5T_4 surfactants in CO₂ solution. While they both lower the CMC, their impact on the mean aggregation number is *opposite*.

B. Shape, size, and density distributions

The radii of gyration give information about the average shape of micelles. The three principle radii of gyration (R_1 , R_2 , and R_3) for the micelles formed in pure H_5T_4 solution are

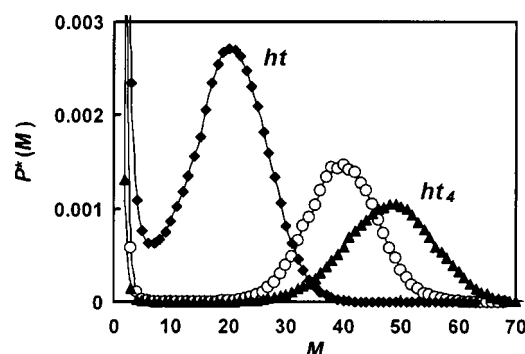


FIG. 7. Number of aggregates per H_5T_4 molecule, $P^*(M) = P(M)/M$, as a function of aggregation number, for the pure H_5T_4 solution (open symbols) and for solutions with 10% ht and 10% ht_4 (closed symbols indicated in the figure) at 2.5% H_5T_4 .

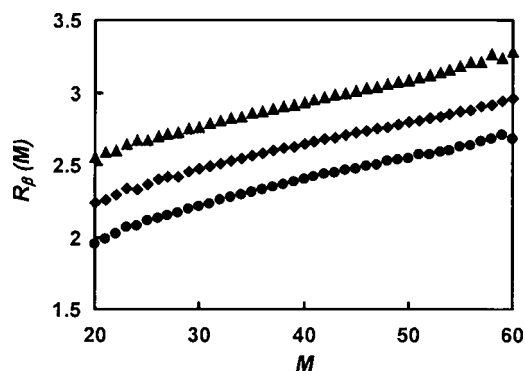


FIG. 8. The three principal radii of gyration R_1 (\bullet), R_2 (\blacklozenge), and R_3 (\blacktriangle) for micelles as a function of aggregation number for 2.5% H_5T_4 surfactant in CO_2 .

plotted as a function of the aggregation number in Fig. 8. As one would expect, the radii of gyration increase monotonously with aggregation number. For the present system, R_1 is about 20% smaller than R_3 , indicating essentially spherical micelles. The behavior of the radii of gyration shown in Fig. 8 is representative for all studied systems, i.e., all micelles in this study are spherical.

The spherical shape of micelles in all systems with and without alcohols is also apparent from snapshots presented in Fig. 9. Closer inspection of the shape of the micelles reveals that the aggregates in the *ht*-containing solution [Fig. 9(b)] have less well defined, i.e., rougher interfaces than micelles in the two other systems. It appears that micelles in the pure H_5T_4 solution [Fig. 9(a)] and in the ht_4 -containing solution [Fig. 9(c)] have approximately the same size, while micelles in the *ht*-containing solution [Fig. 9(b)] are generally smaller. This is consistent with our expectation, since the mean aggregation number in the *ht* containing solution is much smaller than in the other two solutions (see Fig. 5).

For a quantitative comparison of the aggregate sizes, we plot the mean radius of gyration R as a function of aggregation number for the pure, the *ht*-, and the ht_4 -containing systems in Fig. 10(a). At the respective mean aggregation number, micelles in the *ht*-containing solution ($\bar{M}=20$) are considerably smaller than micelles in the pure H_5T_4 solution ($\bar{M}=40$). If ht_4 instead of *ht* is added, then the mean aggregation number increases ($\bar{M}=48$) as well as the size of the micelles.

To study the impact of the addition of alcohol on the size of micelles, one needs to compare micelles of the different solutions having the *same* aggregation number. Micelles in the *ht*-containing solution have slightly larger R values than micelles in the pure H_5T_4 solution, while micelles in the ht_4 -containing solution have slightly lower R values [Fig. 10(a)]. If we consider only the head groups of H_5T_4 to calculate the radius of gyration for the micellar core, R^C , we observe the same trend [Fig. 10(b)]. The micellar size, R , at a given aggregation number increases with the addition of *ht* because of the excluded volume effect caused by binding of *ht* molecules to the micellar core/corona interface. This is consistent with the roughening of the micelle, indicated in the snapshot of the *ht*-containing solution in Fig. 9(b). In

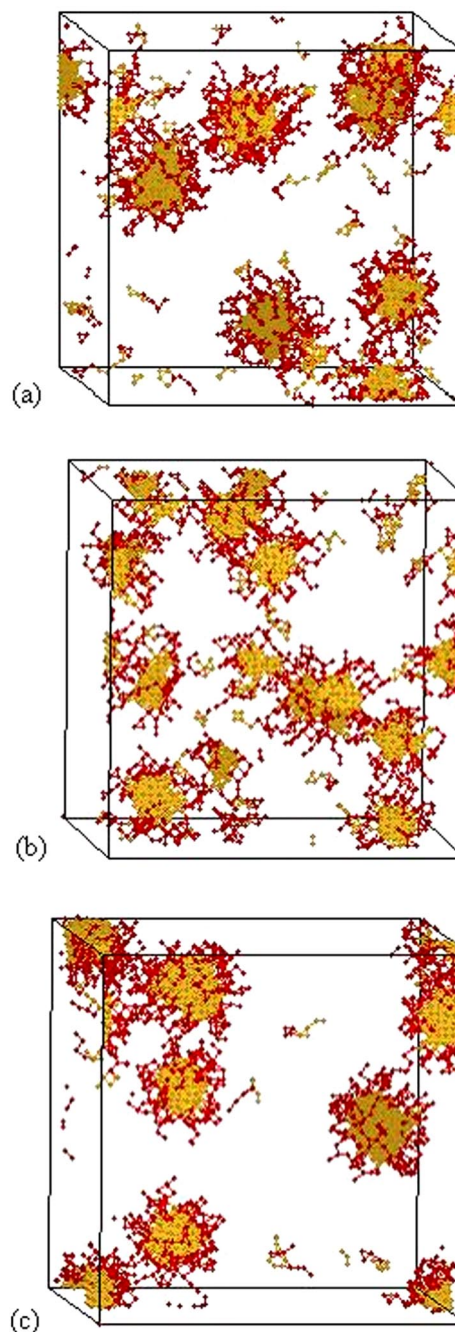


FIG. 9. Snapshots of a 2.5% H_5T_4 solution in a simulation box of $50 \times 50 \times 50$ lattice units containing (a) no alcohol; (b) 10% alcohol *ht*; and (c) 10% alcohol ht_4 . Only surfactant head (yellow) and surfactant tail (red) beads are shown for ease of viewing.

contrast, only a few ht_4 molecules enter the micelles [Fig. 5(b)], causing a smaller excluded volume effect than in the case of *ht*. On the other hand, replacing CO_2 molecules by ht_4 molecules reduces the solvent quality, as can be seen from the interaction parameters in Table I, causing the micelles to become more compact. The net effect is a very small decrease in R [Fig. 10].

A quantitative measure of the sharpness/roughness of the core/corona interface, i.e., the excluded volume effect, is given by the radial density profile of micelles having the

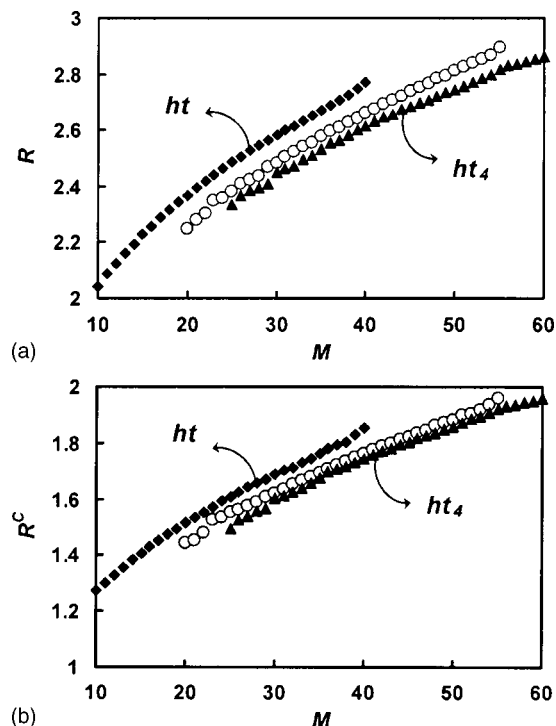


FIG. 10. Mean radius of gyration as a function of aggregation number at 2.5% H_5T_4 for (a) the micelle and (b) the micellar core. Open symbols denote the pure H_5T_4 solution and closed symbols denote the 10% ht - and 10% ht_4 -containing solutions as indicated in the figure. For each solution, only the data range with sufficient sampling is shown.

same aggregation number. As “core/corona interface,” we define the region of r around the inflection point of the density profiles of surfactant head groups, $n_H(r)$, shown in Fig. 11. The weaker decay of $n_H(r)$ for the ht -containing solution compared to the ht_4 -containing solution or the pure H_5T_4

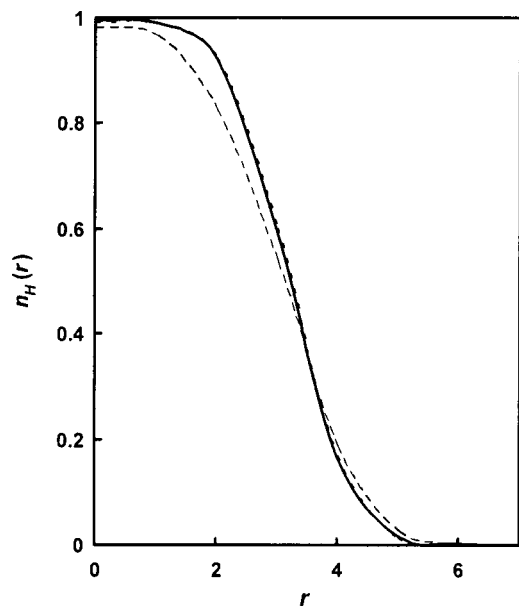


FIG. 11. Radial density profiles of surfactant head groups (H) within micelles of aggregation number $M=35\pm 1$ formed in pure 2.5% H_5T_4 (solid line), with 10% ht added (dashed line) and with 10% ht_4 (dotted line). Note that the curves for the pure system (solid line) and for 10% ht_4 (dotted line) coincide.

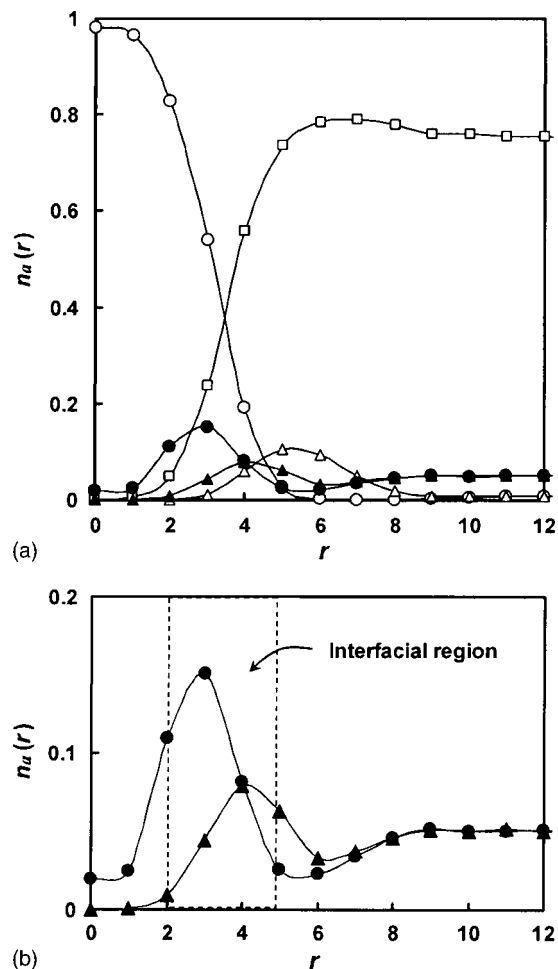


FIG. 12. (a) Radial density profiles for H (\circ), T (\triangle), C (\square), h (\bullet), and t (\blacktriangle) within micelles of aggregation number $M=35\pm 1$ formed in a solution with 2.5% H_5T_4 and 10% ht . (b) same as (a) but only h (\bullet) and t (\blacktriangle) are shown.

solution indicates a less well-defined core/corona interface, i.e., a rougher interface. This roughness is produced by the transfer of surfactant molecules due to the excluded volume effect causing the observed increase of R [see Fig. 10 and Eq. (4)]. The density profiles of surfactant head groups for the ht_4 -containing and the pure H_5T_4 solution are nearly identical, suggesting a negligible impact of ht_4 on the core/corona interface. This is consistent with our earlier observation that only a few ht_4 molecules “enter” the micelles [see Fig. 5(b)].

The complete density profile within micelles formed in the 10% ht -containing solution is shown in Fig. 12(a) and reveals that many ht molecules are located at the core/corona interface. The ht alcohol head groups concentrate at the core side of the interface, while there is a depletion of alcohol head groups in the micellar corona [Fig. 12(b)]. On the other hand, ht tail groups are preferentially located at the corona side of the interface. This indicates a preferential orientation of ht molecules perpendicular to the core/corona interface. The same behavior is observed for the longer alcohols. The concentration of ht head groups close to the interface is much higher than in the surrounding solution. This high

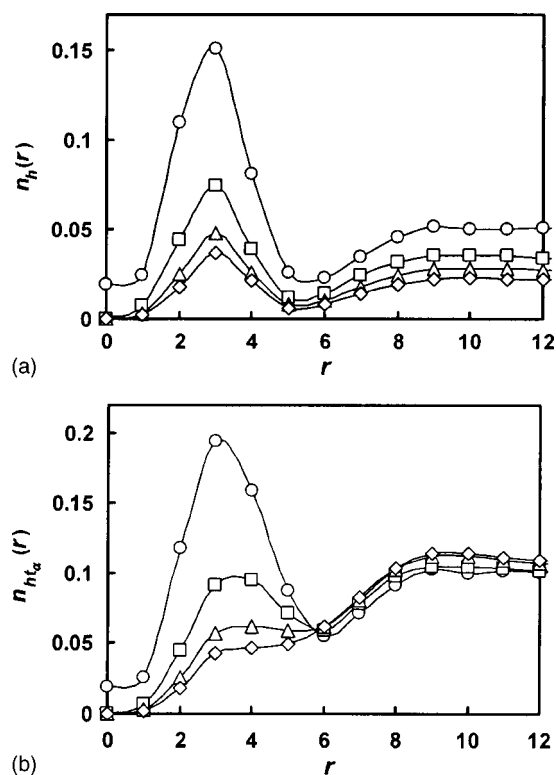


FIG. 13. (a) Radial density profiles of alcohol head groups within micelles of size $M=35\pm 1$ formed in a solution with 2.5% H_5T_4 and 10% ht (\circ), ht_2 (\square), ht_3 (\triangle), or ht_4 (\diamond), respectively. (b) Same as in (a) but for the total of alcohol head and tail groups.

value of ht density is consistent with the earlier observed high number of ht molecules bound in micelles [see Fig. 5(a)].

The density profiles in Fig. 12 suggest that the roughening of the micelle is caused by binding of ht molecules to the interface of the micelles. Such a roughening does not exist in the case of ht_4 . Thus, we expect the density of ht_4 molecules at the interface to be much lower than that of ht molecules. In Fig. 13(a), we compare the density profiles of alcohol head groups for systems containing different alcohols, ht_α . As α increases, one observes a decrease of the head group density at the interface. The value of the density maximum for ht is several times larger than that of ht_4 . This is consistent with our earlier findings presented in Fig. 5 that the mean number of alcohol molecules bound in micelles is several times larger for ht than for ht_4 . We note that (because of the orientation of the cosurfactant molecules perpendicular to the core/corona interface) the total density of cosurfactant head and tail groups at the micellar core/corona interface also decreases with increasing cosurfactant tail length [Fig. 13(b)].

IV. SUMMARY AND CONCLUSIONS

CO_2 is an attractive, environmentally friendly solvent but not a good solvent for polar substances. However, reverse micelles formed by surfactants in CO_2 can incorporate polar molecules. The solubilization capacity of these reverse micelles depends on many factors such as the solubility of the surfactant, the CMC, and the structural properties of the

aggregates. The primary goal of adding additives to a surfactant solution is to increase the solubility of a solute without increasing the concentration of the original surfactant. To choose an appropriate additive, it is necessary to know how additives affect the aggregation behavior of the surfactant solution. As a first step, we have studied the impact of alcohol additives on the self-assembly of the surfactant H_5T_4 in supercritical CO_2 . In particular, we have investigated the dependence of the aggregation behavior on the length, α , of linear alcohols ht_α and their concentration.

All alcohols investigated here decrease the CMC. The effect is stronger the longer the alcohol is. Also for each alcohol, the CMC decreases with increasing alcohol concentration. For ht , we observe that the effect levels off at a concentration of approximately 2.5%. Thus, further increase of the alcohol concentration has little effect on the CMC. If, however, a lower CMC is desired, an alcohol with a longer tail can be used. Clearly, a reduction of the CMC, i.e., micelle formation at lower concentrations, allows solubilization of a solute at lower surfactant concentrations. This is important if the surfactant concentration is limited, e.g., by its own solubility.

While all ht_α alcohols lower the CMC, their impact on the mean aggregation number and the number of aggregates depends strongly on the alcohol chain length α . At 2.5% H_5T_4 , addition of 10% ht_4 causes the aggregation number to increase slightly, whereas the number of aggregates remains constant. In contrast, the number of aggregates doubles and the aggregation number halves if ht is added. In the latter case, ht molecules replace a large number of surfactant molecules in the aggregates. Both effects, an increase in the number of aggregates as well as an increase in aggregation number and size of the micelles, should increase the total amount of solute that can be incorporated in the aggregates. However, there is a striking difference; in the system with more but smaller aggregates, the total surface area per unit volume of solute would be much higher than in the case of a few big micelles. Thus, by changing the length of the alcohol it might be possible to adjust the surface-to-volume ratio of microemulsion droplets.

The main difference in the behavior of ht and ht_4 molecules in the solution is that ht molecules concentrate at the interface of the micelles while ht_4 molecules do not. We believe that the higher loss in configurational entropy of ht_4 compared to ht molecules prevents ht_4 molecules from binding to the micellar core/corona interface. Consequently, ht molecules alter the properties of micelles directly, whereas the effect of ht_4 on the properties of the aggregates is minor. However, the effect of ht_4 on the CMC is large. This CMC reduction arises from the decrease in solvent quality due to the presence of ht_4 molecules. Consequently, ht is a clear cosurfactant while ht_4 would be considered a cosolvent. The transition from one to the other is, however, gradual, as our results for alcohols with intermediate chain length show.

ACKNOWLEDGMENTS

This work was supported by the Department of Energy under Grant No. DE-FG02-98ER14847. We thank the Na-

tional Partnership for Advanced Computational Infrastructure for providing supercomputer time under Grant npa205.

- ¹J. M. DeSimone, *Science* **297**, 799 (2002).
- ²M. M. Jimenez-Carmona and M. D. L. de Castro, *Anal. Chim. Acta* **358**, 1 (1998).
- ³E. L. V. Goetheer, M. A. G. Vorstman, and J. T. F. Keurentjes, *Chem. Eng. Sci.* **54**, 1589 (1999).
- ⁴J. B. McClain, D. E. Betts, D. A. Canelas, E. T. Samulski, J. M. DeSimone, J. D. Londono, H. D. Cochran, G. D. Wignall, D. ChilluraMartino, and R. Triolo, *Science* **274**, 2049 (1996).
- ⁵K. A. Consani and R. D. Smith, *J. Supercrit. Fluids* **3**, 51 (1990).
- ⁶G. J. McFann, Ph.D. thesis, The University of Texas at Austin (1993).
- ⁷G. J. McFann, K. P. Johnston, and S. M. Howdle, *AIChE J.* **40**, 543 (1994).
- ⁸K. Sawada, T. Takagi, and M. Ueda, *Dyes Pigm.* **60**, 129 (2004).
- ⁹J. C. Liu, B. X. Han, G. Z. Li, Z. M. Liu, J. He, and G. Y. Yang, *Fluid Phase Equilib.* **187**, 247 (2001).
- ¹⁰J. C. Liu, B. X. Han, J. L. Zhang, T. C. Mu, G. Z. Li, W. Z. Wu, and G. Y. Yang, *Fluid Phase Equilib.* **211**, 265 (2003).
- ¹¹P. Winsor, *Solvent Properties of Amphiphilic Compounds* (Butterworths, London, 1954).
- ¹²J. L. Salager, "Microemulsions," in *Handbook of Detergents*, edited by G. Broze (Marcel Dekker, New York, 1998).
- ¹³M. J. Rosen, *Surfactants and Interfacial Phenomena* (Wiley, New York, 1978).
- ¹⁴A. Graciaa, J. Lachaise, C. Cucuphat, M. Bourrel, and J. L. Salager, *Langmuir* **9**, 669 (1993).
- ¹⁵A. Graciaa, J. Lachaise, C. Cucuphat, M. Bourrel, and J. L. Salager, *Langmuir* **9**, 3371 (1993).
- ¹⁶M. Miñana-Perez, A. Graciaa, J. Lachaise, and J. L. Salager, *Colloids Surf., A* **100**, 217 (1995).
- ¹⁷J. L. Salager, A. Graciaa, and J. Lachaise, *J. Surfactants Deteg.* **1**, 403 (1998).
- ¹⁸K. Shinoda, "The Formation of Micelles," in *Colloidal Surfactants*, edited by K. Shinoda, T. Nakagawa, B. Tamamushi, and T. Isemura (Academic, New York, 1963).
- ¹⁹A. Castedo, J. L. Del Castillo, M. J. Suarez-Fillo, and J. R. Rodriguez, *J. Colloid Interface Sci.* **196**, 148 (1997).
- ²⁰D. J. Jobe, R. E. Verrall, B. Skalski, and E. Aicart, *J. Phys. Chem.* **96**, 6811 (1992).
- ²¹D. J. Mitchell and B. W. Ninham, *J. Chem. Soc., Faraday Trans. 2* **77**, 601 (1981).
- ²²M. J. Hou and D. O. Shah, *Langmuir* **3**, 1086 (1987).
- ²³V. K. Bansal, D. O. Shah, and J. P. Oconnell, *J. Colloid Interface Sci.* **75**, 462 (1980).
- ²⁴P. G. Degennes and C. Taupin, *J. Phys. Chem.* **86**, 2294 (1982).
- ²⁵N. Asgharian, P. Otken, C. Sunwoo, and W. H. Wade, *Langmuir* **7**, 2904 (1991).
- ²⁶M. Kahlweit, R. Strey, and G. Busse, *J. Phys. Chem.* **95**, 5344 (1991).
- ²⁷G. Palazzo, F. Lopez, M. Giustini, G. Colafemmina, and A. Ceglie, *J. Phys. Chem. B* **107**, 1924 (2003).
- ²⁸S. Salaniwal, S. T. Cui, H. D. Cochran, and P. T. Cummings, *Langmuir* **17**, 1773 (2001).
- ²⁹S. Salaniwal, S. T. Cui, H. D. Cochran, and P. T. Cummings, *Langmuir* **17**, 1784 (2001).
- ³⁰S. Senapati, J. S. Keiper, J. M. DeSimone, G. D. Wignall, Y. B. Melnichenko, H. Frielinghaus, and M. L. Berkowitz, *Langmuir* **18**, 7371 (2002).
- ³¹S. R. P. da Rocha, K. P. Johnston, and P. J. Rossky, *J. Phys. Chem. B* **106**, 13250 (2002).
- ³²M. Lisal, C. K. Hall, K. E. Gubbins, and A. Z. Panagiotopoulos, *J. Chem. Phys.* **116**, 1171 (2002).
- ³³L. F. Scanu, K. E. Gubbins, and C. K. Hall, *Langmuir* **20**, 514 (2004).
- ³⁴L. Rekvig, B. Hafskjold, and B. Smit, *J. Chem. Phys.* **120**, 4897 (2004).
- ³⁵M. Zaldivar and R. G. Larson, *Langmuir* **19**, 10434 (2003).
- ³⁶R. G. Larson, L. E. Scriven, and H. T. Davis, *J. Chem. Phys.* **83**, 2411 (1985).
- ³⁷R. G. Larson, *J. Chem. Phys.* **89**, 1642 (1988).
- ³⁸R. G. Larson, *J. Phys. II* **6**, 1441 (1996).
- ³⁹M. Lisal, C. K. Hall, K. E. Gubbins, and A. Z. Panagiotopoulos, *Mol. Simul.* **29**, 139 (2003).
- ⁴⁰D. Frenkel and B. Smit, *Understanding Molecular Simulation: From Algorithms to Applications* (Academic, London, 1996).
- ⁴¹J. Hoshen and R. Kopelman, *Phys. Rev. B* **14**, 3438 (1976).
- ⁴²J. N. Israelachvili, D. J. Mitchell, and B. W. Ninham, *J. Chem. Soc., Faraday Trans. 2* **72**, 1525 (1976).
- ⁴³C. Tanford, *The Hydrophobic Effect: Formation of Micelles and Biological Membranes* (Wiley, New York, 1980), pp. 90–95.
- ⁴⁴E. Ruckenstein and R. Nagarajan, *J. Phys. Chem.* **79**, 2622 (1975).
- ⁴⁵S. K. Talsania, Y. M. Wang, R. Rajagopalan, and K. K. Mohanty, *J. Colloid Interface Sci.* **190**, 92 (1997).
- ⁴⁶S. K. Talsania, L. A. Rodriguez-Guadarrama, K. K. Mohanty, and R. Rajagopalan, *Langmuir* **14**, 2684 (1998).
- ⁴⁷M. A. Floriano, E. Caponetti, and A. Z. Panagiotopoulos, *Langmuir* **15**, 3143 (1999).
- ⁴⁸A. Z. Panagiotopoulos, M. A. Floriano, and S. K. Kumar, *Langmuir* **18**, 2940 (2002).
- ⁴⁹J. Rudnick and G. Gaspari, *Science* **237**, 384 (1987).
- ⁵⁰A. D. Mackie, A. Z. Panagiotopoulos, and S. K. Kumar, *J. Chem. Phys.* **102**, 1014 (1995).
- ⁵¹Note that in Ref. 50 the temperature scale is given in units of $|w_{CV}^*| = \frac{1}{2}|e_{CC}^*|$.